Volume 1, Issue 1, Pages 1–20

Journal of Applied Mathematics and Computational Research (JAMCR)

Journal homepage: https://smcrjournals.org

Numerical Investigation of a Non-Singular Fractional Mathematical Model for HIV Infection of CD4$^+$ T Cells with KellerSegel Chemotaxis

Pappu Verma[1], Sachin Kumar[2,*]

[1,2]Department of Mathematics, Government Degree College, Budaun, Uttar Pradesh, India

[*]Corresponding author: sachinraghav522@gmail.com

Article history:

Received: 15 April 2026

Revised: 06 May 2026

Accepted: 05 June 2026

Available online: 30 June 2026

Article type:

Research Article

Keywords:

Keller-Segel equations

Fractional PDE

Mittag-Leffler kernel fractional derivative

Model for HIV infection of CD4$^+$ T-cells

spectral method

Abstract

In this study, we introduce an efficient numerical approach for solving time-fractional differential equations that use the Atangana-Baleanu fractional derivative with the Mittag-Leffler kernel. We showcase the applicability of the proposed method via two representative time-fractional models: the HIV infection model that represents the dynamics of CD4+ T-cells and the Keller-Segel chemotaxis model. The first step of the procedure involves creating a numerical approximation for the Atangana-Baleanu fractional derivative and employing it to develop the Legendre operational matrix of fractional differential approximation. Once the proposed operational matrix is created, along with Legendre spectral collocation method, the governing fractional differential equation along with the associated initial and boundary conditions are converted into a system of nonlinear algebraic equations that we later solve to obtain solutions. Several numerical examples were presented in order to evaluate the effectiveness of the method developed and the obtained numerical results closely coincided with the correlated exact solutions that proved the correctness, efficiency, and proficiency of the proposed method of solving nonlinear time-fractional differential equations using the Mittag-Leffler kernel.

1. Introduction

Fractional calculus has emerged as a significant branch of mathematical analysis that extends the classical concepts of differentiation and integration to arbitrary real or complex orders. Owing to its ability to incorporate memory and hereditary characteristics into mathematical models, fractional calculus has become an indispensable tool for describing a wide range of complex phenomena encountered in science and engineering. Comprehensive treatments of the theory and applications of fractional calculus can be found in [1, 2, 3].

During the past two decades, fractional differential equations (FDEs) have attracted considerable attention because they provide more accurate mathematical descriptions of many real-world processes than their integer-order counterparts. Applications of FDEs span numerous disciplines, including control theory, stochastic processes, biomedical engineering, finance, economics, viscoelasticity, groundwater flow, signal processing, and many other branches of applied science. Consequently, the development of efficient and reliable numerical techniques for solving fractional models has become an active area of research.

Several definitions of fractional derivatives have been proposed in the literature, among which the Riemann–Liouville, Caputo, Riesz, Hadamard, and Grnwald–Letnikov operators are the most widely used. More recently, variable-order fractional derivatives have received increasing attention because the order of differentiation is allowed to vary with space, time, or other physical variables. Such operators provide greater modeling flexibility by capturing memory effects that evolve during the underlying physical process. Variable-order fractional models have therefore found important applications in anomalous diffusion, heterogeneous media, reaction–diffusion systems, and advection–diffusion phenomena. Interested readers are referred to [4] for applications of variable-order fractional reaction–diffusion and advection–diffusion equations.

Although fractional mathematical models often provide a more realistic representation of physical systems, obtaining their analytical solutions is generally difficult and, in many practical situations, impossible. This challenge has stimulated extensive research on the development of efficient numerical algorithms for solving fractional differential equations [5, 6, 7, 8, 9]. Among the available numerical techniques, spectral methods based on operational matrices have gained widespread popularity because of their high accuracy, rapid convergence, and computational efficiency. Various operational matrix formulations have been developed using orthogonal basis functions and wavelets, including Haar wavelets, Legendre wavelets [12], Chebyshev wavelets [13], Laguerre polynomials [14], Legendre polynomials [15], and semi-orthogonal Genocchi polynomials [16]. Other widely used numerical approaches include the Adomian decomposition method [11], homotopy perturbation method [17], fractional differential transform method [18], predictor–corrector method [19], and generalized block pulse operational matrix method [20].

In recent years, fractional derivatives with non-singular kernels have attracted significant interest because they overcome certain limitations associated with classical singular-kernel operators while providing improved descriptions of memory-dependent processes. Among these operators, the Atangana–Baleanu fractional derivative employs a non-singular Mittag–Leffler kernel, whereas the Caputo–Fabrizio derivative is characterized by a non-singular exponential kernel. Motivated by the attractive mathematical properties of the Atangana–Baleanu operator, the present work employs the Atangana–Baleanu–Caputo (ABC) fractional derivative to develop an efficient numerical framework for solving systems of fractional differential equations and fractional partial differential equations.

To demonstrate the effectiveness of the proposed methodology, two representative mathematical models are investigated. The first model describes the dynamics of HIV infection in $CD4^+$ T-cells. Human Immunodeficiency Virus (HIV) primarily infects and destroys $CD4^+$ T-cells, progressively weakening the immune system and eventually leading to Acquired Immunodeficiency Syndrome (AIDS) [22]. The concentration of $CD4^+$ T-cells is therefore regarded as one of the most important clinical indicators for monitoring disease progression. In healthy individuals, the concentration of $CD4^+$ T-cells typically ranges from 800 to 1200 mm^{-3}. These cells are continuously generated from precursors in the bone marrow and thymus at a production rate r, undergo natural death at rate β, and proliferate through mitosis at rate p [23]. Their population dynamics can be described by the logistic growth equation [24, 25, 26, 27]

$$\frac{dT}{dt} = r - \beta T + pT\left(1 - \frac{T}{T_{\max}}\right), \tag{1}$$

where T denotes the concentration of healthy $CD4^+$ T-cells and $T_{\max}$ represents their maximum carrying capacity. During HIV infection, the total T-cell population consists of healthy and infected cells, denoted by $T + T^*$, where T^* represents the infected $CD4^+$ T-cell population.

The second model considered in this work is the time-fractional Keller–Segel chemotaxis system, which has been widely employed to describe the collective movement of biological cells in response to chemical concentration gradients. Both mathematical models serve as important benchmark problems for assessing the accuracy and computational efficiency of the proposed numerical method.

The remainder of the paper is organized as follows. Section 2 presents the fundamental definitions and mathematical properties of the Caputo, Riemann–Liouville, and Atangana–Baleanu–Caputo fractional derivatives. In Section 3, a novel operational matrix of fractional differentiation with the Mittag–Leffler kernel is derived using shifted Legendre polynomials. Section 4 describes the proposed numerical algorithm and its implementation for solving the considered models. Numerical experiments together with error analysis are presented in Section 5 to demonstrate the effectiveness of the proposed approach. Finally, the main conclusions and possible directions for future research are summarized in Section 6.

2. Preliminaries on Fractional Integrals and Derivatives

3. Mathematical Preliminaries

This section summarizes the essential concepts of fractional calculus that are required for the subsequent development of the proposed numerical algorithm. In particular, we recall the definitions of the Riemann–Liouville and Caputo fractional operators together with the Atangana–Baleanu–Caputo fractional derivative involving the non-singular Mittag–Leffler kernel.

3.1 Classical Fractional Operators

The Riemann–Liouville fractional integral provides the foundation for several fractional differential operators.

Definition 2.1. Let $f(\tau) \in L^1(0,\infty)$ and let $\alpha > 0$. The left-sided Riemann–Liouville fractional integral is defined by

$$(I^\alpha f)(\tau) = \frac{1}{\Gamma(\alpha)} \int_0^\tau (\tau-\eta)^{\alpha-1} f(\eta)\, d\eta. \tag{2}$$

The associated Riemann–Liouville fractional derivative is defined as follows.

Definition 2.2. Suppose that $m-1 < \alpha < m$, where $m = 1, 2, \ldots$. Then

$$^{RL}D_\tau^\alpha f(\tau) = \frac{d^m}{d\tau^m} I^{m-\alpha} f(\tau). \tag{3}$$

The Caputo fractional derivative is extensively employed in engineering and applied sciences because it naturally accommodates classical initial conditions.

Definition 2.3. For $m-1 < \alpha < m$, the Caputo fractional derivative is given by

$$^{C}D_\tau^\alpha f(\tau) = \frac{1}{\Gamma(m-\alpha)} \int_0^\tau (\tau-\zeta)^{m-\alpha-1} f^{(m)}(\zeta)\, d\zeta. \tag{4}$$

When $\alpha = m$, the above expression reduces to the ordinary derivative,

$$^{C}D_\tau^m f(\tau) = f^{(m)}(\tau).$$

Moreover,

$$^{C}D_\tau^\mu c = 0, \tag{5}$$

where c denotes an arbitrary constant.

For $\lambda \geq 0$,

$$^{C}D_\tau^\mu \tau^\lambda = \begin{cases} 0, & \lambda < m-1, \\ \dfrac{\Gamma(\lambda+1)}{\Gamma(\lambda-\mu+1)} \tau^{\lambda-\mu}, & \lambda \geq m-1. \end{cases} \tag{6}$$

The Caputo operator satisfies the superposition principle,

$$^{C}D_\tau^\mu (a_1 f_1 + a_2 f_2) = a_1 {}^{C}D_\tau^\mu f_1 + a_2 {}^{C}D_\tau^\mu f_2, \tag{7}$$

where a_1 and a_2 are constants.

Furthermore,

$$I^\mu \left(^{C}D_\tau^\mu f \right) = f(\tau) - \sum_{r=0}^{m-1} \frac{f^{(r)}(0)}{r!} \tau^r, \tag{8}$$

provided that $f \in AC^m[0,T]$.

3.2 Atangana–Baleanu–Caputo Fractional Derivative

The Atangana–Baleanu–Caputo derivative is characterized by a non-singular Mittag–Leffler kernel and has become an important operator for modeling hereditary phenomena.

Definition 2.4 [28, 29]. Let $u(x,\tau)$ be sufficiently smooth and let $0 < \nu < 1$. Then

$$ {}_{0}^{ABC}D_{\tau}^{\nu}u(x,\tau) = \frac{M(\nu)}{1-\nu}\int_0^{\tau} \frac{\partial u(x,\eta)}{\partial \eta} E_{\nu}\left(-\frac{\nu}{1-\nu}(\tau-\eta)^{\nu}\right) d\eta, \tag{9} $$

where the normalization function satisfies

$$ M(0) = M(1) = 1, $$

and

$$ E_{\nu}(z) = \sum_{r=0}^{\infty} \frac{z^r}{\Gamma(\nu r + 1)}. $$

The ABC fractional operator possesses a non-local and non-singular kernel, allowing it to describe long-memory processes more accurately than many classical fractional operators. Consequently, it has found extensive applications in diffusion theory, viscoelasticity, biological systems, thermal transport, fluid mechanics, and many other areas of applied science.

4. Construction of the Operational Matrix for the Mittag–Leffler Fractional Derivative

4.1 Numerical Approximation of the ABC Fractional Derivative of Monomial Basis Functions

In this section, we derive a numerical approximation for the Atangana–Baleanu–Caputo (ABC) fractional derivative of monomial basis functions. The proposed approximation forms the basis for constructing the operational matrix of fractional differentiation developed in this work. Since the integral representation of the ABC fractional derivative contains the non-singular Mittag–Leffler kernel, an analytical evaluation is generally unavailable. Therefore, a composite Simpson quadrature rule is employed to obtain an accurate numerical approximation of the corresponding integral operator.

Theorem 3.1. Let

$$ g(x) = x^p, \qquad p \in \mathbb{N}_0, $$

and let the fractional order satisfy

$$ m-1 < \nu < m, \qquad m = 1, 2, \ldots. $$

For $p \geq m$, the Atangana–Baleanu–Caputo fractional derivative of $g(x)$ can be approximated by

$$
\begin{aligned}
{}_0^{ABC}D_x^{\nu} x^p \approx & \frac{\mathcal{B}(\nu)}{m-\nu} \frac{p!}{(p-m)!} \frac{\Delta x}{3} \Bigg[\Psi_{\nu,p}(\zeta_0, x) + \Psi_{\nu,p}(\zeta_N, x) \\
& + 4 \sum_{\substack{i=1 \\ i \text{ odd}}}^{N-1} \Psi_{\nu,p}(\zeta_i, x) + 2 \sum_{\substack{i=2 \\ i \text{ even}}}^{N-2} \Psi_{\nu,p}(\zeta_i, x) \Bigg],
\end{aligned} \tag{10}
$$

where

$$\Psi_{\nu,p}(\zeta, x) = \zeta^{p-m} E_{\nu} \left(-\frac{\nu}{m-\nu} (x-\zeta)^{\nu} \right). \tag{11}$$

Proof.

If $p < m$, then

$$\frac{d^m}{dx^m} x^p = 0,$$

which immediately implies

$${}_0^{ABC}D_x^{\nu} x^p = 0.$$

Hence, only the case $p \geq m$ needs to be considered. According to the definition of the Atangana–Baleanu–Caputo fractional derivative,

$${}_0^{ABC}D_x^{\nu} x^p = \frac{\mathcal{B}(\nu)}{m-\nu} \int_0^x \frac{d^m}{d\zeta^m}(\zeta^p) E_{\nu} \left(-\frac{\nu}{m-\nu} (x-\zeta)^{\nu} \right) d\zeta. \tag{12}$$

Using the elementary identity

$$\frac{d^m}{d\zeta^m}(\zeta^p) = \frac{p!}{(p-m)!} \zeta^{p-m},$$

the above equation becomes

$${}_0^{ABC}D_x^{\nu} x^p = \frac{\mathcal{B}(\nu)}{m-\nu} \frac{p!}{(p-m)!} \int_0^x \zeta^{p-m} E_{\nu} \left(-\frac{\nu}{m-\nu} (x-\zeta)^{\nu} \right) d\zeta. \tag{13}$$

For convenience, define the kernel function

$$\Psi_{\nu,p}(\zeta, x) = \zeta^{p-m} E_{\nu} \left(-\frac{\nu}{m-\nu} (x-\zeta)^{\nu} \right). \tag{14}$$

Therefore,

$${}_0^{ABC}D_x^{\nu} x^p = \frac{\mathcal{B}(\nu)}{m-\nu} \frac{p!}{(p-m)!} \int_0^x \Psi_{\nu,p}(\zeta, x)\, d\zeta. \tag{15}$$

Since the above integral cannot generally be evaluated in closed form, a numerical quadrature formula is employed. Let the interval $[0, x]$ be partitioned into N equal subintervals with mesh size

$$\Delta x = \frac{x}{N},$$

and nodal points

$$\zeta_i = i\Delta x, \qquad i = 0, 1, \ldots, N.$$

Applying the composite Simpson rule yields

$$\begin{aligned}\int_0^x \Psi_{\nu,p}(\zeta,x)\,d\zeta \approx & \frac{\Delta x}{3}\Bigg[\Psi_{\nu,p}(\zeta_0,x)+\Psi_{\nu,p}(\zeta_N,x) \\ & + 4\sum_{\substack{i=1 \\ i \text{ odd}}}^{N-1}\Psi_{\nu,p}(\zeta_i,x) + 2\sum_{\substack{i=2 \\ i \text{ even}}}^{N-2}\Psi_{\nu,p}(\zeta_i,x)\Bigg].\end{aligned} \tag{16}$$

Substituting this approximation into the previous equation immediately gives

$$\begin{aligned}{}_0^{ABC}D_x^{\nu} x^p \approx & \frac{\mathcal{B}(\nu)}{m-\nu}\frac{p!}{(p-m)!}\frac{\Delta x}{3}\Bigg[\Psi_{\nu,p}(\zeta_0,x)+\Psi_{\nu,p}(\zeta_N,x) \\ & + 4\sum_{\substack{i=1 \\ i \text{ odd}}}^{N-1}\Psi_{\nu,p}(\zeta_i,x) + 2\sum_{\substack{i=2 \\ i \text{ even}}}^{N-2}\Psi_{\nu,p}(\zeta_i,x)\Bigg],\end{aligned} \tag{17}$$

which establishes the desired approximation.

□

The above approximation provides an efficient numerical evaluation of the ABC fractional derivative of polynomial basis functions. Since the operational matrix developed in the subsequent subsection is constructed from these monomial approximations, the proposed formulation significantly reduces the computational complexity associated with the evaluation of fractional operators involving the Mittag–Leffler kernel. Moreover, the use of the composite Simpson quadrature ensures high-order numerical accuracy while preserving computational efficiency, making the proposed technique suitable for solving a broad class of fractional differential and fractional partial differential equations.

4.2 Shifted Legendre polynomial and their basic properties

This section contains some basic properties of orthogonal Legendre polynomial which has been shifted to the interval $[0,1]$ from $[-1,1]$. We use these properties in the derivation of Legendre operational matrix of fractional differentiation in Atangana-Baleanu derivative sense. The following equation is corresponds to the series form of shifted Legendre polynomial of degree p

$$\mathit{\Psi}_i(y) = \sum_{k=0}^{p} \frac{(-1)^{p+k}(p+k)!}{(k!)^2(l-k)!} y^k, \tag{18}$$

where $p = 0, 1, \cdots$. The orthogonal condition is changed to as according to the shift of Legendre polynomial.

$$\int_0^1 \mathit{\Psi}_j(y)\mathit{\Psi}_i(y) = \begin{cases} \frac{1}{2i+1}, & p = j, \\ 0 & p \neq j. \end{cases} \tag{19}$$

We can approximate a function $u(y) \in L^2[0,1]$ in terms of shifted Legendre polynomial

$$u(y) = u_N(y) = \sum_{j=0}^{N} a_j \mathit{\Psi}_i(y), \tag{20}$$

where

$$a_j = (2j+1)\int_0^1 u(y)\Psi_j(y). \tag{21}$$

In case of a function of two variable the approximation is as follows

$$u(y,t) = \sum_{p=0}^{N-1}\sum_{l=0}^{N-1} a_{pl}\Psi_p(y)\Psi_l(t), \tag{22}$$

where a_{il} coefficient. We can rewrite equation (14) in matrix form as

$$u(y) = u_N(y) = \sum_{p=0}^{N-1}\sum_{l=0}^{N-1} a_{il}\Psi_l(t)\Psi_p(y) = \Pi_N^T(y)\mathbf{A}^T\Pi_N(t), \tag{23}$$

where

$$\begin{aligned} &\mathbf{A}^T = (a_0, a_1, \cdots, a_{N-1}),\\ &\Pi_N(y) = (\Psi_0(y), \Psi_1(y), \cdots, \Psi_{N-1}(y))^T. \end{aligned} \tag{24}$$

Theorem 2: Let $\Pi_N(\zeta)$ represent the shifted Legendre vector, then Mittag-Leffler kernel fractional differentiation of this vector can be approximated in terms of operational matrix as

$${}_0^{ABC}D_t^{\upsilon}\Pi_N(t) = Q^{\upsilon}\Pi_N(t), \tag{25}$$

where $n-1<\upsilon<n$ and Q^{υ} represents the fractional differentiation operational matrix $N\times N$ size of order υ in ABC sense. It is given by

$$Q^{\upsilon} = \begin{bmatrix} 0 & 0 & \cdots & 0\\ 0 & 0 & \cdots & 0\\ \vdots & \vdots & \cdots & \vdots\\ \sum_{\iota=\lceil\upsilon\rceil}^{\lceil\upsilon\rceil}\varsigma_{\lceil\upsilon\rceil,\iota,1} & \sum_{\iota=\lceil\upsilon\rceil}^{\lceil\upsilon\rceil}\varsigma_{\lceil\upsilon\rceil,0,\iota} & \cdots & \sum_{\iota=\lceil\upsilon\rceil}^{\lceil\upsilon\rceil}\varsigma_{\lceil\upsilon\rceil,m-1,\iota}\\ \vdots & \vdots & \cdots & \vdots\\ \sum_{\iota=\lceil\upsilon\rceil}^{i}\varsigma_{i,0,\iota} & \sum_{\iota=\lceil\upsilon\rceil}^{i}\varsigma_{i,1,\iota} & \cdots & \sum_{\iota=\lceil\upsilon\rceil}^{i}\varsigma_{i,m-1,\iota}\\ \vdots & \vdots & \cdots & \vdots\\ \sum_{\iota=\lceil\upsilon\rceil}^{m-1}\varsigma_{m-1,0,\iota} & \sum_{\iota=\lceil\upsilon\rceil}^{m-1}\varsigma_{m-1,1,\iota} & \cdots & \sum_{\iota=\lceil\upsilon\rceil}^{m-1}\varsigma_{m-1,m-1,\iota}. \end{bmatrix},$$

and the value of the term $\varsigma_{i,j,\iota}$ is given by following relation

$$\begin{aligned} \varsigma_{i,j,\iota} =& \iota(\iota-1)\cdots(\iota-(n-1))\frac{(-1)^{\iota+i}(\iota+i)!}{(-\iota+l)!(\iota!)^2}\times(2j+1)\\ &\times\frac{B(\upsilon)}{(-\upsilon+n)}\sum_{l=0}^{j}\frac{(-1)^{j+l}(j+l)!}{(-l+j)!(l!)^2}\times(\lambda_0+\lambda_1+\cdots+\lambda_M) \end{aligned}$$

.

Proof: The approximation of fractional derivative of polynomial function t^{ι} is as (Theorem 1)

$$
\begin{aligned}
{}_0^{ABC}D_t^{\upsilon}t^{\iota} = \iota(\iota-1)\cdots(\iota-(n-1)) \times \frac{B(\upsilon)}{n-\upsilon} \times \frac{h}{3}\Big[&M_{\upsilon,\iota}(s_0,t) + M_{\upsilon,\iota}(s_m,t) \\
&+ 4\{M_{\upsilon,\iota}(s_1,t) + M_{\upsilon,\iota}(s_3,t) + \cdots + M_{\upsilon,\iota}(s_{m-1},t)\} \\
&+ 2\{M_{\upsilon,\iota}(s_2,t) + M_{\upsilon,\iota}(s_4,t) + \cdots + M_{\upsilon,\iota}(s_{m-2},t)\}\Big].
\end{aligned}
$$

Applying the fractional derivative of non-singular type (Mittag-Leffler kernel fractional derivative) of order υ on the series from of shifted Legendre polynomial of degree i, we have

$$
{}_0^{ABC}D_t^{\upsilon}\psi_i(t) = \sum_{\iota=0}^{i} \frac{(-1)^{i+\iota}(i+\iota)!}{(\iota!)^2(l-\iota)!} \times {}_0^{ABC}D_t^{\upsilon}t^{\iota}, \quad i = 0,1,2,3,\cdots
$$

$$
\begin{aligned}
= \sum_{\iota=\lceil\upsilon\rceil}^{i} \iota(\iota-1)\cdots(\iota-(n-1))\frac{(-1)^{\iota+i}(\iota+i)!}{(-\iota+l)!(\iota!)^2} \times \frac{B(\upsilon)}{-\upsilon+n} \times \frac{h}{3}\Big[&M_{\upsilon,\iota}(s_0,t) \\
+ 2\{M_{\upsilon,\iota}(s_2,t) + M_{\upsilon,\iota}(s_4,t) + \cdots + M_{\upsilon,\iota}(s_{m-2},t)\}& \\
+ 4\{M_{\upsilon,\iota}(s_1,t) + M_{\upsilon,\iota}(s_3,t) + \cdots + M_{\upsilon,\iota}(s_{m-1},t)\} + M_{\upsilon,\iota}(s_m,t)\Big]&.
\end{aligned}
$$

The value of ABC derivative of Legendre vector is approximated as a linear combination of orthogonal Legendre polynomial to find out the $(i,j)^{th}$ element named as $\rho_{i,j}$ of matrix of differentiation Q^{α}

$$
\begin{aligned}
{}_0^{ABC}D_t^{\alpha}\psi_i(t) &= \sum_{j=0}^{m-1} \rho_{i,j}\psi_j(t), \\
\rho_{i,j} &= \langle {}_0^{ABC}D_t^{\alpha}\psi_i(t), \psi_j(t)\rangle
\end{aligned}
\tag{26}
$$

$$
\begin{aligned}
= \sum_{\iota=\lceil\upsilon\rceil}^{i} \frac{(-1)^{\iota+i}(\iota+i)!}{(-\iota+l)!(\iota!)^2}\iota(\iota-1)\cdots(\iota-(n-1)) \times \frac{B(\upsilon)}{-\upsilon+n} \times \frac{h}{3}\Big[&\langle M_{\upsilon,\iota}(s_0,t), \psi_j(t)\rangle \\
+ \langle M_{\upsilon,\iota}(s_M,t), \psi_j(t)\rangle& \\
+ 2\{\langle M_{\upsilon,\iota}(s_2,t), \psi_j(t)\rangle + \langle M_{\upsilon,\iota}(s_4,t), \psi_j(t)\rangle + \cdots + \langle M_{\upsilon,\iota}(s_{M-2},t), \psi_j(t)\rangle\}& \\
+ 4\{\langle M_{\upsilon,\iota}(s_1,t), \psi_j(t)\rangle + \langle M_{\upsilon,\iota}(s_3,t), \psi_j(t)\rangle + \cdots + \langle M_{\upsilon,\iota}(s_{M-1},t), \psi_j(t)\rangle\}\Big]&.
\end{aligned}
\tag{27}
$$

The evaluation of inner products appearing in above expression is as follows

$$
\langle M_{\upsilon,\iota}(s_p,t), \psi_j(t)\rangle = (2j+1)\int_0^1 M_{\upsilon,\iota}(s_p,t)\psi_j(t)dt, \quad p = 0,1,\cdots M \tag{28}
$$

$$
= (2j+1)\int_0^1 M_{\upsilon,\iota}(s_p,t)\sum_{l=0}^{j}\frac{(j+l)!(-1)^{j+l}}{(l!)^2(-l+j)!}t^l dt
$$

$$
= (2j+1)\sum_{l=0}^{j}\frac{(-1)^{j+l}(j+l)!}{(l!)^2(j-l)!}\Big(\int_0^1 M_{\upsilon,\iota}(s_p,t)t^l dt\Big)
$$

$$
\begin{aligned}
=&(2j+1)\sum_{l=0}^{j}\frac{h}{3}\Big[2\{M_{\upsilon,\iota}(s_p,t_2){t_2}^l+M_{\upsilon,\iota}(s_p,t_4){t_4}^l+\cdots+M_{\upsilon,\iota}(s_p,t_{M-2})t_(M-2)^l\}\\
&+M_{\upsilon,\iota}(s_p,t_0){t_0}^l+M_{\upsilon,\iota}(s_p,t_M){t_M}^l\\
&+4\{M_{\upsilon,\iota}(s_p,t_1){t_1}^l+M_{\upsilon,\iota}(s_p,t_3){t_3}^l+\cdots+M_{\upsilon,\iota}(s_p,t_{M-1})t_(M-1)^l\}\Big]\\
&\times\frac{(-1)^{j+l}}{(-l+j)!}\times\frac{(j+l)!}{(l!)^2}\\
&=\sum_{l=0}^{j}\frac{(-1)^{j+l}}{(-l+j)!}\times\frac{(j+l)!}{(l!)^2}\times\lambda_p\times(2j+1),
\end{aligned}
$$

where

$$
\begin{aligned}
\lambda_p=&\frac{h}{3}\Big[2\{M_{\upsilon,\iota}(s_p,t_2){t_2}^l+M_{\upsilon,\iota}(s_p,t_4){t_4}^l+\cdots+M_{\upsilon,\iota}(s_p,t_{M-2})t_(M-2)^l\}\\
&+M_{\upsilon,\iota}(s_p,t_0){t_0}^l+M_{\upsilon,\iota}(s_p,t_M){t_M}^l\\
&+4\{M_{\upsilon,\iota}(s_p,t_1){t_1}^l+M_{\upsilon,\iota}(s_p,t_3){t_3}^l+\cdots+M_{\upsilon,\iota}(s_p,t_{M-1})t_(M-1)^l\}\Big].
\end{aligned}
$$

The value $\rho_{i,j}$ is obtained by putting in place of inner products in equation (19) as

$$
\begin{aligned}
\rho_{i,j}=&\sum_{\iota=\lceil\upsilon\rceil}^{i}\frac{B(\upsilon)}{n-\upsilon}\frac{(-1)^{i+\iota}(i+\iota)!}{(\iota!)^2(l-\iota)!}\times\iota(\iota-1)\cdots(\iota-(n-1))\\
&\times(2j+1)\sum_{l=0}^{j}\frac{(-1)^{j+l}}{(-l+j)!}\times\frac{(j+l)!}{(l!)^2}\times\times(2j+1)\times(\lambda_0+\lambda_1+\cdots+\lambda_M).
\end{aligned}
\tag{29}
$$

$$
\begin{aligned}
\rho_{i,j}=&\sum_{l=0}^{j}\sum_{\iota=\lceil\upsilon\rceil}^{i}(2j+1)\frac{(-1)^{j+l}}{(-l+j)!}\times\frac{(j+l)!}{(l!)^2}\times\frac{B(\upsilon)}{n-\upsilon}\frac{(-1)^{i+\iota}(i+\iota)!}{(\iota!)^2(l-\iota)!}\times\iota(\iota-1)\cdots(\iota-(n-1))\\
&\times(2j+1)\times(\lambda_0+\lambda_1+\cdots+\lambda_M).
\end{aligned}
\tag{30}
$$

If we consider $\rho_{i,j}=\sum_{\lceil\upsilon\rceil}^{i}\varsigma_{i,j,\iota}$, then get

$$
\begin{aligned}
\varsigma_{i,j,\iota}=&\frac{B(\upsilon)}{n-\upsilon}\frac{(-1)^{i+\iota}(i+\iota)!}{(\iota!)^2(l-\iota)!}\times\iota(\iota-1)\cdots(\iota-(n-1))\\
&\times(2j+1)\sum_{l=0}^{j}\frac{(-1)^{j+l}}{(-l+j)!}\times\frac{(j+l)!}{(l!)^2}\times\times(2j+1)\times(\lambda_0+\lambda_1+\cdots+\lambda_M).
\end{aligned}
$$

$$
\begin{aligned}
\varsigma_{i,j,\iota}=&\sum_{l=0}^{j}\times(2j+1)\frac{(-1)^{j+l}}{(-l+j)!}\times\frac{(j+l)!}{(l!)^2}\frac{B(\upsilon)}{n-\upsilon}\frac{(-1)^{i+\iota}(i+\iota)!}{(\iota!)^2(l-\iota)!}\times\iota(\iota-1)\cdots(\iota-(n-1))\\
&\times(2j+1)\times(\lambda_0+\lambda_1+\cdots+\lambda_M).
\end{aligned}
$$

The above derived operational matrix is for fractional order. As we also used the integer order derivative in our model so there is a need of operational matrix of integer order which is defined by the following expression

$$\rho_{i,j} = \begin{cases} 2 \times (2j+1), & j = -\iota + i, \\ 0, & j \neq -\iota + i, \end{cases} \tag{31}$$

where the value of ι depends on the value of m.

5. Error estimation

Theorem 3: Let us consider a function $g(\zeta)$ defined on interval $[0, L]$ which is n^{th} times continuously differentiable and $g_n(\zeta)$ be the best approximation of $g(\zeta)$ then we have

$$\|g(\zeta) - g_n(\zeta)\| \leq \frac{S^{n+1}M}{(n+1)!}\sqrt{L}, \tag{32}$$

where

$$M = \max_{\zeta \in [0,1]} g^{n+1}(\zeta), \quad S = \max\{L - x_0, x_0\}.$$

Proof: The function $g(\zeta)$ can be expanded in the series form by using Taylor expansion,

$$g(\zeta) = g(x_0) + (\zeta - x_0)g'(x_0) + \cdots + \frac{(\zeta - x_0)^n}{n!}g^n(x_0) + \frac{(\zeta - x_0)^{n+1}}{n!}g^{n+1}(\chi), \tag{33}$$

where $x_0 \in [0, L], \quad \chi \in (x_0, \zeta)$. We consider

$$\hat{g}_n(\zeta) = g(x_0) + (\zeta - x_0)g'(x_0) + \cdots + \frac{(\zeta - x_0)^n}{n!}g^n(x_0). \tag{34}$$

So from above equations we have

$$\|g(\zeta) - \hat{g}_n(\zeta)\| = |\frac{(\zeta - x_0)^{n+1}}{(n+1)!}g^{n+1}(\chi)|. \tag{35}$$

We know $g_n(\zeta)$ is the best approximation of $g(\zeta)$ then we have

$$\begin{aligned} \|g(\zeta) - g_n(\zeta)\|^2 &\leq \|g(\zeta) - \hat{g}_n(\zeta)\|^2 \\ &= \int_0^L \omega(t)\|g(\zeta) - \hat{g}_n(\zeta)\|^2 dx \end{aligned} \tag{36}$$

$$\begin{aligned} &= \int_0^L \omega(\zeta)\Big(|\frac{(\zeta - x_0)^{n+1}}{(n+1)!}g^{n+1}(\chi)|\Big)^2 dx \\ &\leq \frac{M^2}{((n+1)!)^2}\int_0^L \omega(\zeta)\Big((\zeta - x_0)^{n+1}\Big)^2 dx. \end{aligned}$$

Considering, $S = \max\{L = x_0, x_0\}$ and we get the following result

$$\begin{aligned} \|g(\zeta) - g_n(\zeta)\|^2 &\leq \frac{M^2(S^{n+1})^2}{((n+1)!)^2} \int_0^L \omega(\zeta) dx \\ &= \frac{M^2(S^{n+1})^2}{((n+1)!)^2} L. \end{aligned} \tag{37}$$

Taking square root we get the required result (28).

6. Investigated model and proposed method for numerical solution

This section is devoted to find out approximate solution of a system of FDEs. First, we consider the following fractional model for HIV infection of CD4$^+$

$$\begin{aligned} &{}_0^{ABC}D_t^{\zeta} T(t) = r \times T\Big(1 - \frac{T+I}{T_{max}}\Big) - kVT - \alpha T + p, \\ &{}_0^{ABC}D_t^{\eta} I(t) = -\beta I + kVT, \\ &{}_0^{ABC}D_t^{\mu} V(t) = -\gamma V + \beta N I. \end{aligned} \tag{38}$$

The following initial conditions are considered for above model

$$\begin{aligned} T(0) &= T_0, \\ I(0) &= I_0, \\ V(0) &= V_0. \end{aligned} \tag{39}$$

The values of parameters and lowing initial conditions are

$$\begin{aligned} &I_0 = 0, T_0 = 0.1, V_0 = 0.1, \alpha = 0.02, p = 0.1 \\ &k = 0.0027, N = 10, T_{max} = 1500, \beta = 0.3, \gamma = 0.3. \end{aligned}$$

We adopt the collocation method together with Legendre collocation method to find the numerical solution of model (23). The unknown quantities present in the model $T(t)$, $I(t)$ and $V(t)$ are approximated in series form of Legendre polynomial as

$$T(t) = \sum_{i=0}^{N-1} a_i \psi_i(t), I(t) = \sum_{i=0}^{N-1} b_i \psi_i(t), V(t) = \sum_{i=0}^{N-1} c_i \psi_i(t), \tag{40}$$

where a_i, b_i and c_i are coefficients which are to be determined for $i = 0, 2, \cdots$.
The above approximations can be modified with the help of matrix representation of approximation as follows

$$T(t) = A.\Pi_N(t), I(t) = B.\Pi_N(t), V(t) = C.\Pi_N(t), \tag{41}$$

where $A = [a_{ij}]_{1\times N}, B = [b_{ij}]_{1\times N}$ and $C = [c_{ij}]_{1\times N}$ is an row vector of unknowns and $\Pi_N(\zeta) =$

$(\psi_0(\zeta), \psi_1(\zeta), \cdots, \psi_{N-1}(\zeta))^T$ correspond to a column vector. The ABC fractional derivatives of the unknown quantities in terms of operational matrix are given by

$$\begin{aligned}
{}_0^{ABC}D_t^{\zeta}T(t) &= A.Q^{\zeta}.\Pi_N(t),\\
{}_0^{ABC}D_t^{\eta}I(t) &= B.Q^{\eta}.\Pi_N(t),\\
{}_0^{ABC}D_t^{\mu}V(t) &= C.Q^{\mu}.\Pi_N(t).
\end{aligned} \tag{42}$$

Similarly, the approximation of boundary and initial conditions in terms of operational matrix is as follows:

$$\begin{aligned}
A.\Pi_N(0) &= T_0(0),\\
B.\Pi_N(0) &= I_0(0),\\
C.\Pi_N(0) &= V_0(0).
\end{aligned} \tag{43}$$

The residual functions are obtained with the help of equations $(26) - (28)$:

$$\begin{aligned}
\xi_1(\zeta, t) &= A.Q^{\zeta}.\Pi_N(t) - r \times A.\Pi_N\Big(1 - \frac{A.\Pi_N + B.\Pi_N}{T_{max}}\Big) + kA.\Pi_N C.\Pi_N + \alpha A.\Pi_N - p,\\
\xi_2(\zeta, t) &= B.\Pi_N + \beta B.\Pi_N - kA.\Pi_N C.\Pi_N,\\
\xi_3(\zeta, t) &= C.\Pi_N + \gamma C.\Pi_N - \beta N B.\Pi_N.
\end{aligned} \tag{44}$$

Now collocating (34) and (35) at Legendre nodes in the interval $[0, 1]$, we get nonlinear system of algebraic equations. The solution is obtained by solving these algebraic equations and finding the unknowns C.

The parabolic system due to Keller and Segel characterizes the aggregation process of cellular slime model by chemical attraction. The system of Keller-Segel equations can be written as follows

$$\begin{aligned}
{}_0^{ABC}D_t^{\varphi}v(\zeta, t) &= s_1\frac{\partial^2 v(\zeta, t)}{\partial \zeta^2} - \frac{\partial}{\partial \zeta}\Big(v(\zeta, t)\frac{\partial \chi(\varrho)}{\partial \zeta}\Big),\\
{}_0^{ABC}D_t^{\psi}\varrho(\zeta, t) &= s_2\frac{\partial^2 \varrho(\zeta, t)}{\partial \zeta^2} + s_3\varrho(\zeta, t) - s_4\varrho(\zeta, t).
\end{aligned} \tag{45}$$

We take the following boundary and initial conditions

$$\begin{aligned}
&\frac{\partial v(0, t)}{\partial \zeta} = \frac{\partial v(1, t)}{\partial \zeta} = \frac{\partial \varrho(0, t)}{\partial \zeta} = \frac{\partial \varrho(1, t)}{\partial \zeta} = 0,\\
&v(\zeta, 0) = v_0(\zeta),\\
&\varrho(\zeta, 0) = \varrho_0(\zeta).
\end{aligned} \tag{46}$$

Here, the functions $v(\zeta, t)$ and $\varrho(\zeta, t)$ represent the concentration of amoebae and the concentration of a chemical substance. The function $\chi(\varrho)$ denotes the sensitivity function. Chemotactic term is represented by the expression $\frac{\partial}{\partial \zeta}\Big(v(\zeta, t)\frac{\partial \chi(\varrho)}{\partial \zeta}\Big)$ which characterizes that the cells are sensitive to chemicals and attracted by them. Functions of two variables $v(\zeta, t)$ and $\varrho(\zeta, t)$ is approximated with the help of shifted Legendre polynomial as

$$\begin{aligned} v(\zeta,t) &= \sum_{i=0}^{N-1}\sum_{j=0}^{N-1} d_{ij}\psi_i(\zeta)\psi_j(t), \\ \varrho(\zeta,t) &= \sum_{i=0}^{N-1}\sum_{j=0}^{N-1} e_{ij}\psi_i(\zeta)\psi_j(t), \end{aligned} \tag{47}$$

where c_{ij} are unknown coefficients for $i = 0, 2, \cdots$; and $j = 0, 1, 2, \cdots$. The matrix form of above approximations are

$$\begin{aligned} v(\zeta,t) &= \Pi_N^T(\zeta).D.\Pi_N(t), \\ \varrho(\zeta,t) &= \Pi_N^T(\zeta).E.\Pi_N(t), \end{aligned} \tag{48}$$

where $\Pi_N(\zeta) = (\psi_0(\zeta), \psi_1(\zeta), \cdots, \psi_{N-1}(\zeta))^T$ represents a column vector and $D = [c_{ij}]_{N\times N}$, $E = [c_{ij}]_{N\times N}$ corresponds to the $N \times N$ matrices of unknowns. With the help of Theorem 2, the derived operational matrix of non-singular fractional derivative of orders φ and ψ on (33) respectively with respect to the variable t, the approximation of fractional derivative of unknowns are

$$\begin{aligned} {}_0^{ABC}D_t^{\varphi} v(t,\zeta) &= \Pi_N(\zeta)^T.D.Q^{\varphi}.\Pi_N(t), \\ {}_0^{ABC}D_t^{\psi} \varrho(t,\zeta) &= \Pi_N(\zeta)^T.E.Q^{\varphi}.\Pi_N(t). \end{aligned} \tag{49}$$

Similarly, the approximation of boundary and initial conditions with the help of operational matrix can be as

$$\begin{aligned} &Q^1\Pi_N^T(0).D.\Pi_N(t) = 0, Q^1\Pi_N^T(0).D.\Pi_N(t) = 0, \\ &Q^1\Pi_N^T(0).E.\Pi_N(t) = 0, Q^1\Pi_N^T(1).E.\Pi_N(t) = 0, \\ &\Pi_N^T(0).E.\Pi_N(t) = 0, \Pi_N^T(0).E.\Pi_N(t) = 0. \end{aligned} \tag{50}$$

The residual functions for Keller-Segel model are obtained as with the help of equations (33) − (35) as

$$\begin{aligned} &\kappa_1(\zeta,t) = Q^1\Pi_N(\zeta)^T.D.\Pi_N(t)Q^1\Pi_N(\zeta)^T.E.\Pi_N(t) \\ &+ \Pi_N(\zeta)^T.D.\Pi_N(t)Q^2\Pi_N(\zeta)^T.E.\Pi_N(t) \\ &+ \Pi_N(\zeta)^T.D.Q^{\varphi}.\Pi_N(t) - s_1Q^2\Pi_N(\zeta)^T.D.\Pi_N(t) \\ &+ \kappa_2(\zeta,t) = \Pi_N(\zeta)^T.E.Q^{\varphi}.\Pi_N(t) - s_2Q^2\Pi_N(\zeta)^T.D.\Pi_N(t) \\ &- s_3\Pi_N(\zeta)^T.D.\Pi_N(t) + -s_4\Pi_N(\zeta)^T.E.\Pi_N(t). \end{aligned} \tag{51}$$

The solution of model is obtained by collocating these residual functions at Legendre nodes and finding the value of unknown matrices D and E.

7. Numerical results and validation

This section contains the numerical validation of our method. This is done by comparing our numerical results with the exact ones for the particular cases of our models. The feasibility of method can be seen through by the error graphs and tables.

Example 1: For $\zeta = 0.9$, $\eta = 0.9$ and $\mu = 0.9$, the following model of HIV infection of $CD4^+$:

$$\begin{aligned}
{}_0^{ABC}D_t^{\zeta}T(t) &= r \times T\Big(1 - \frac{T+I}{T_{max}}\Big) - kVT - \alpha T + p + m_1(t),\\
{}_0^{ABC}D_t^{\eta}I(t) &= -\beta I + kVT + m_2(t),\\
{}_0^{ABC}D_t^{\mu}V(t) &= -\gamma V + \beta N I + m_3(t).
\end{aligned} \tag{52}$$

We take the following initial conditions for particular problem 1

$$\begin{aligned}
T(0) &= 0.1,\\
I(0) &= 0,\\
V(0) &= 0.1.
\end{aligned} \tag{53}$$

Choose $m_i(t)$, $i = 1, 2, 3$ in such a way that the exact analytical solution of above given problem is $T(t) = t^2 + 0.1$, $I(t) = t^4$, and $V(t) = t^5 + 0.1$.

The absolute error plot between the exact solution and derived approximation solution for $T(t)$, $I(t)$, and $V(t)$ at $N = 4$ is presented here (Figure 1, Figure 2 and Figure 3). We see the accuracy of our method from these error graphs. This proves that our method is suitable for the system of fractional ordinary differential equation with time-fractional Mittag-Leffler non-singular kernel.

Table 1: Variations of absolute errors

T(t) ↓	I(t)	V(t)
3.2×10^{-5}	9.9×10^{-5}	5.5×10^{-6}
2.7×10^{-5}	3.4×10^{-4}	2.1×10^{-5}
6.4×10^{-5}	3.7×10^{-4}	3.4×10^{-5}
1.8×10^{-5}	4.7×10^{-4}	3.3×10^{-5}
5.2×10^{-5}	6.4×10^{-4}	7.6×10^{-5}
5.4×10^{-5}	7.1×10^{-3}	4.1×10^{-5}
1.1×10^{-5}	5.7×10^{-3}	6.4×10^{-5}
7.2×10^{-5}	6.1×10^{-4}	9.7×10^{-5}

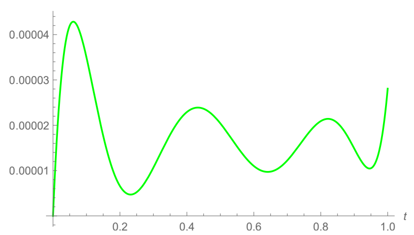

Figure 1: Variation of absolute error between derived numerical results and the exact ones for the unknown $T(t)$ taking $N = 4$.

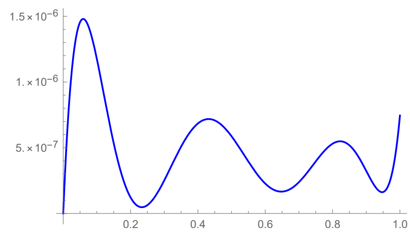

Figure 2: Variation of absolute error between derived numerical results and the exact ones for the unknown $I(t)$ taking $N = 4$.

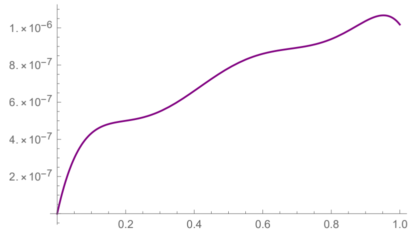

Figure 3: Variation of absolute error between derived numerical results and the exact ones for the unknown $V(t)$ taking $N = 4$.

Example 2: Letting $\varphi = 0.9$, $\chi = 0.9$, $s_1 = s_2 = s_3 = s_4 = 1$ and sensitivity function $\chi(\varrho) = 0$, consider the following Mittag-Leffler kernel time fractional linear Keller-Segel equation:

$$\begin{aligned}
{}_0^{ABC}D_t^{\varphi} v(\zeta,t) &= \frac{\partial^2 v(\zeta,t)}{\partial \zeta^2} + f_1(\zeta,t), \\
{}_0^{ABC}D_t^{\psi} \varrho(\zeta,t) &= \frac{\partial^2 \varrho(\zeta,t)}{\partial \zeta^2} + \varrho(\zeta,t) - \varrho(\zeta,t) + f_2(\zeta,t).
\end{aligned} \tag{54}$$

subject to initial and boundary conditions:

$$\begin{aligned}
&\frac{\partial v(0,t)}{\partial \zeta} = \frac{\partial v(1,t)}{\partial \zeta} = \frac{\partial \varrho(0,t)}{\partial \zeta} = \frac{\partial \varrho(1,t)}{\partial \zeta} = 0, \\
&v(\zeta,0) = \zeta^2(\zeta-1)^2, \\
&\varrho(\zeta,0) = 0.
\end{aligned} \tag{55}$$

The two variable function $v(\zeta,t) = \zeta^2(\zeta-1)^2 e^t$, $\varrho(\zeta,t) = \zeta^2(\zeta-1)^2 t$ is corresponds to the exact solution of above problem. Here the force functions $f_1(\zeta,t)$ and $f_2(\zeta,t)$ can be derived by putting the value of exact solution in given system.

The $3D$-plot of absolute error between numerical and exact solutions with $N = 4$, is depicted by Figure 4.

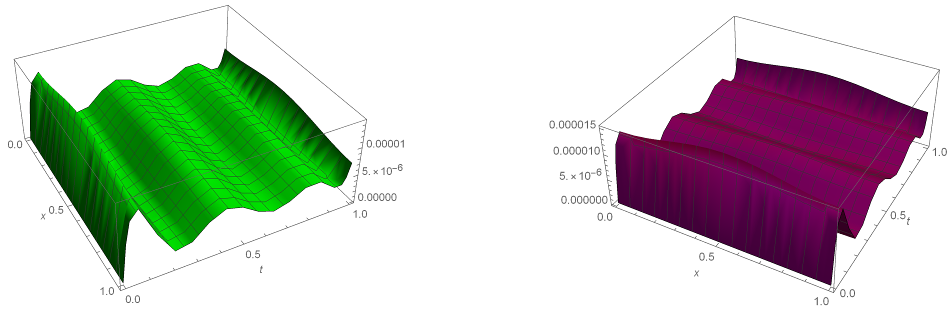

(a) (b)

Figure 4: Plots of absolute error for $v(\zeta,t)$ and $\varrho(\zeta,t)$ for $N=4$.

Example 3: For $\varphi = 0.9$, $\psi = 0.9$, $s_1 = s_2 = s_3 = s_4 = 1$ and sensitivity function $\chi(\varrho) = \varrho$, we consider get Keller Segel model with Mittag-Leffler time fractional derivative

$$
\begin{aligned}
{}_0^{ABC}D_t^{\varphi} v(\zeta,t) &= \frac{\partial^2 v(\zeta,t)}{\partial \zeta^2} - \frac{\partial}{\partial \zeta}\Big(v(\zeta,t)\frac{\partial \varrho}{\partial \zeta}\Big),\\
{}_0^{ABC}D_t^{\psi} \varrho(\zeta,t) &= \frac{\partial^2 \varrho(\zeta,t)}{\partial \zeta^2} + v(\zeta,t) - \varrho(\zeta,t).
\end{aligned}
\tag{56}
$$

The initial and boundary conditions are taken as follows

$$
\begin{aligned}
&\frac{\partial v(0,t)}{\partial \zeta} = \frac{\partial v(1,t)}{\partial \zeta} = \frac{\partial \varrho(0,t)}{\partial \zeta} = \frac{\partial \varrho(1,t)}{\partial \zeta} = 0,\\
&v(\zeta,0) = v_0(\zeta),\\
&\varrho(\zeta,0) = \varrho_0(\zeta).
\end{aligned}
\tag{57}
$$

The exact solution is $v(\zeta,t) = \zeta^3(\zeta-1)^3 e^t$ and $\varrho(\zeta,t) = \zeta^3(\zeta-1)^3 t^2$.
The absolute error $3D$ plots between numerical and exact solutions are presented in Figure 5 for the Keller Segel model. The error figures validated our method for a system of fractional PDE system having time-fractional Mittag-Leffler non-singular kernel. We can easily predict the good accuracy of our method for time fractional PDE system of equations with Mittag-Leffler kernel.

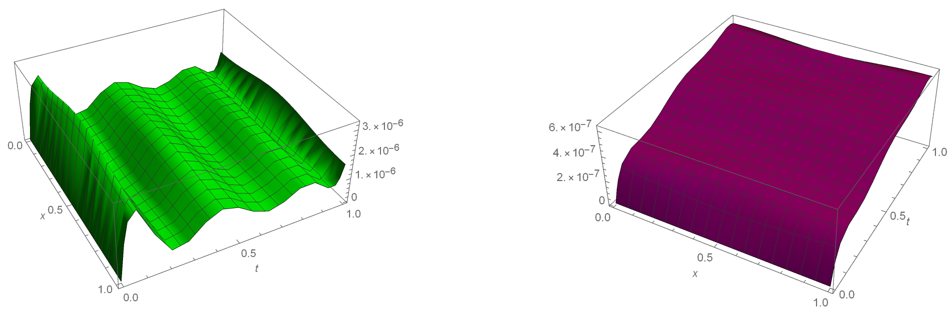

(a) (b)

Figure 5: Plots of absolute error for $v(\zeta,t)$ and $\varrho(\zeta,t)$ for $N=4$.

8. Conclusion

This paper proposes a numerical method for the analysis of systems of nonlinear fractional differential equations which utilise the Atangana-Baleanu-Caputo (ABC) fractional operator with the Mittag-Leffler kernel. In particular, the paper studies two models which exhibit the time-fractional behaviour: the model of HIV infection based on $CD4^+$ T-cells and the chemotactic Keller-Segel model. The numerical approach is based on collocation and makes use of a newly derived ABC Legendre operational matrix. The operational matrix allows the fractional differential equations to be transformed into a system of algebraic equations where the solutions can be computed effectively. The numerical results show that the method is able to provide very accurate solutions and is therefore reliable. The validity of the method is further confirmed using error analysis and graphical comparison of the results obtained for both models. The findings demonstrate that the method is effective in solving systems of nonlinear fractional differential equations that involve the ABC operator and that it can solve many other complicated fractional dynamical systems.

References

[1] A. Kilbas, H. Srivastava, J.J.Trujillo, Theory and Applications of the Fractional Differential Equations, Vol. 204, Elsevier (North- Holland), Amsterdam Amsterdam, 2006.

[2] I. Podlubny, Fractional differential equations, to methods of their solution and some of their applications, Fractional Differential Equations: An Introduction to Fractional Derivatives, Academic Press, San Diego, CA.

[3] J. T. Machado, V. Kiryakova, F. Mainardi, Recent history of fractional calculus, Communications in nonlinear science and numerical simulation 16 (3) (2011) 1140–1153.

[4] S. Kumar, P. Pandey, S. Das, Gegenbauer wavelet operational matrix method for solving variable-order non-linear reaction–diffusion and galilei invariant advection–diffusion equations, Computational and Applied Mathematics 38 (4) (2019) 162.

[5] M. Alqhtani, K. M. Owolabi, K. M. Saad, Spatiotemporal (target) patterns in sub-diffusive predator-prey system with the caputo operator, Chaos, Solitons & Fractals 160 (2022) 112267.

[6] H. M. Srivastava, K. M. Saad, W. M. Hamanah, Certain new models of the multi-space fractal-fractional kuramoto-sivashinsky and korteweg-de vries equations, Mathematics 10 (7) (2022) 1089.

[7] M. Alqhtani, K. M. Saad, Numerical solutions of space-fractional diffusion equations via the exponential decay kernel, AIMS Mathematics 7 (4) (2022) 6535–6549.

[8] K. M. Saad, Fractal-fractional brusselator chemical reaction, Chaos, Solitons & Fractals 150 (2021) 111087.

[9] M. Alqhtani, K. M. Saad, R. Shah, W. Weera, W. M. Hamanah, Analysis of the fractional-order local poisson equation in fractal porous media, Symmetry 14 (7) (2022) 1323.

[10] Y. Li, W. Zhao, Haar wavelet operational matrix of fractional order integration and its applications in solving the fractional order differential equations, Applied Mathematics and Computation 216 (8) (2010) 2276–2285.

[11] L. Suarez, A. Shokooh, An eigenvector expansion method for the solution of motion containing fractional derivatives, Journal of Applied Mechanics-transactions of The Asme - J APPL MECH 64.

[12] H. Jafari, S. Yousefi, M. Firoozjaee, S. Momani, C. M. Khalique, Application of legendre wavelets for solving fractional differential equations, Computers & Mathematics with Applications 62 (3) (2011) 1038–1045.

[13] L. Yuanlu, Solving a nonlinear fractional differential equation using chebyshev wavelets, Communications in Nonlinear Science and Numerical Simulation 15 (9) (2010) 2284–2292.

[14] B. Gürbüz, M. Sezer, Laguerre polynomial solutions of a class of initial and boundary value problems arising in science and engineering fields, Acta Physica Polonica A 130 (1) (2016) 194–197.

[15] Z. Odibat, On legendre polynomial approximation with the vim or ham for numerical treatment of nonlinear fractional differential equations, Journal of Computational and Applied Mathematics 235 (9) (2011) 2956–2968.

[16] S. Kumar, P. Pandey, S. Das, Operational matrix method for solving nonlinear space-time fractional order reaction-diffusion equation based on genocchi polynomial, Special Topics & Reviews in Porous Media: An International Journal 11 (1).

[17] I. Hashim, O. Abdulaziz, S. Momani, Homotopy analysis method for fractional ivps, Communications in Nonlinear Science and Numerical Simulation 14 (3) (2009) 674–684.

[18] P. Darania, A. Ebadian, A method for the numerical solution of the integro-differential equations, Applied Mathematics and Computation 188 (2007) 657–668.

[19] K. Diethelm, N. J. Ford, A. D. Freed, A predictor-corrector approach for the numerical solution of fractional differential equations, Nonlinear Dynamics 29 (1-4) (2002) 3–22.

[20] Y. Li, N. Sun, Numerical solution of fractional differential equations using the generalized block pulse operational matrix, Computers & Mathematics with Applications 62 (3) (2011) 1046–1054.

[21] A. Atangana, J. Gómez-Aguilar, Numerical approximation of riemann-liouville definition of fractional derivative: From Riemann-Liouville to Atangana-Baleanu, Numerical Methods for Partial Differential Equations 34 (5) (2018) 1502–1523.

[22] C. M. Pinto, A. R. Carvalho, The hiv/tb coinfection severity in the presence of tb multi-drug resistant strains, Ecological complexity 32 (2017) 1–20.

[23] A. Jajarmi, D. Baleanu, A new fractional analysis on the interaction of HIV with CD4+ t-cells, Chaos, Solitons & Fractals 113 (2018) 221–229.

[24] A. Atangana, E. Alabaraoye, Solving a system of fractional partial differential equations arising in the model of hiv infection of CD4+ cells and attractor one-dimensional keller-segel equations, Advances in Difference Equations 2013 (1) (2013) 94.

[25] L. Wang, M. Y. Li, Mathematical analysis of the global dynamics of a model for hiv infection of CD4+ t cells, Mathematical Biosciences 200 (1) (2006) 44–57.

[26] B. Asquith, C. R. Bangham, The dynamics of t-cell fratricide: application of a robust approach to mathematical modelling in immunology, Journal of theoretical biology 222 (1) (2003) 53–69.

[27] M. Y. Ongun, The laplace adomian decomposition method for solving a model for hiv infection of CD4+ t cells, Mathematical and Computer Modelling 53 (5-6) (2011) 597–603.

[28] A. Atangana, I. Koca, Chaos in a simple nonlinear system with atangana–baleanu derivatives with fractional order, Chaos, Solitons & Fractals 89 (2016) 447–454.

[29] A. Atangana, M. A. Khan, Validity of fractal derivative to capturing chaotic attractors, Chaos, Solitons & Fractals 126 (2019) 50–59.